Magnetic Resonance Imaging 55 (2019) 46–51

Contents lists available at ScienceDirect

Magnetic Resonance Imaging

journal homepage: www.elsevier.com/locate/mri

Original contribution

The rotating stretched curved planar reconstruction of 3D-FIESTA MR imaging for evaluating the anterior cruciate ligament of the knee joint☆,☆☆

Jun Zhang[a], Dapeng Hao[a,*], Feng Duan[a], Tengbo Yu[c], Chuanyu Zhang[a], Junyi Che[b]

[a] The Department of Radiology, The Affiliated Hospital of Qingdao University, Qingdao, 266003, China
[b] The Department of Radiology, Qingdao Municipal Hospital, Qingdao 266003, China
[c] Department of Sports Medicine, The Affiliated Hospital of Qingdao University, Qingdao, 266003, China

ARTICLE INFO

Keywords:
Anterior cruciate ligament
Magnetic resonance imaging
Curved planar reconstruction

ABSTRACT

Purpose: To determine the feasibility of the rotating stretched curved planar reconstruction (CPR) of three-dimensional fast imaging with steady-state acquisition magnetic resonance imaging (3D-FIESTA MRI) for evaluating the anterior cruciate ligament of the knee joint.

Materials and methods: MRI of 40 knee joints in healthy volunteers was performed on a 3.0-T MR scanner and a phased-array extremity coil. The protocol consisted of oblique sagittal spin echo (SE) T1WI, coronal FS-PDWI, axial FS-FSE-T2WI, and 3D-FIESTA sequences. The rotating stretched curved planar reconstructions (CPR) of the ACL at angles of 0°, 30°, 60°, 90°, 120°, 150°, and 180° were generated from images of 3D-FIESTA sequences. Signal-to-noise ratio (SNR) and contrast-to-noise ratio (CNR) of the 3D-FIESTA were compared with those of the oblique sagittal SE T1WI sequence. The presence of the tibial attachment, midportion, femoral attachment, and double bundles of the ACL on the oblique sagittal SE T1WI and CPR of 3D-FIESTA MR imaging were divided into two categories: visible and not visible.

Results: The ACL SNR efficiency of 3D-FIESTA sequences was significantly higher than that of oblique sagittal SE T1WI sequence ($P < 0.05$). The 3D-FIESTA sequences produced images with a significantly higher CNR between ACL and synovial fluid than did the oblique sagittal SE T1WI sequence ($P < 0.05$). CPR of 3D-FIESTA MRI generated an excellent visualization of the ACL. The CPR of 3D-FIESTA MRI was rated superior to oblique sagittal SE T1WI sequence in 60% and 65% of cases with regard to the tibial attachment and midportion of ACL, respectively ($P < 0.05$). CPR of 3D-FIESTA MR imaging was rated superior to oblique sagittal SE T1WI sequence in 80% and 85% of cases with regard to femoral attachment and double bundles of ACL, respectively ($P < 0.05$).

Conclusion: The rotating stretched curved planar reconstruction of 3D-FIESTA sequences is significantly better than that of conventional 2D-MRI in evaluating the native ACL and its components, AM bundle and PL bundle, in healthy volunteers.

1. Introduction

The anterior cruciate ligament (ACL) runs an oblique course from its origin at the medial side of the lateral femoral condyle, traverses through the distal–anterior–medial aspect of the intercondylar fossa and terminates at the medial tibial eminence [1,2]. The ACL of the knee has a double bundle structure of anteromedial (AM) and posterolateral (PL) fibers, which are based on the insertion of both individual bundles into the tibial surface (Fig. 1) [3,4]. The double-bundle structure of the ACL is crucial to the stabilization of the knee [5] and it plays a key role in controlling the transmission of large compressive and shear intersegmental forces across the knee [6].

Abbreviations: FIESTA, fast imaging with steady-state acquisition; ACL, anterior cruciate ligament; AMB, anteromedial bundle; PLB, posterolateral bundle; MPR, multiplanar reformat; CPR, curved planar reconstruction; FOV, field of view; ROI, region of interest; SNR, signal-to-noise ratio; CNR, contrast to Noise Ratio; CNs, central nervous system; SSFP, steady-state free precession; MEDIC GRE, multiple-echo data image combination gradient echo; VISTA, volume isotropic turbo spin-echo acquisition; FSE-Cube, fast spin echo; WE-DESS, water excitation double-echo steady state; LSD, Least Significant Difference

☆ There is no any conflict of interest information for all authors.

☆☆ This topic was presented at RNSA 2012 (see Annex 1 for details).

* Corresponding author at: Department of Radiology, The Affiliated Hospital of Qingdao University, 16, Jiangsu Road, Qingdao 266003, China.
E-mail address: haodp_2009@163.com (D. Hao).

https://doi.org/10.1016/j.mri.2018.09.013
Received 2 May 2018; Received in revised form 9 September 2018; Accepted 13 September 2018

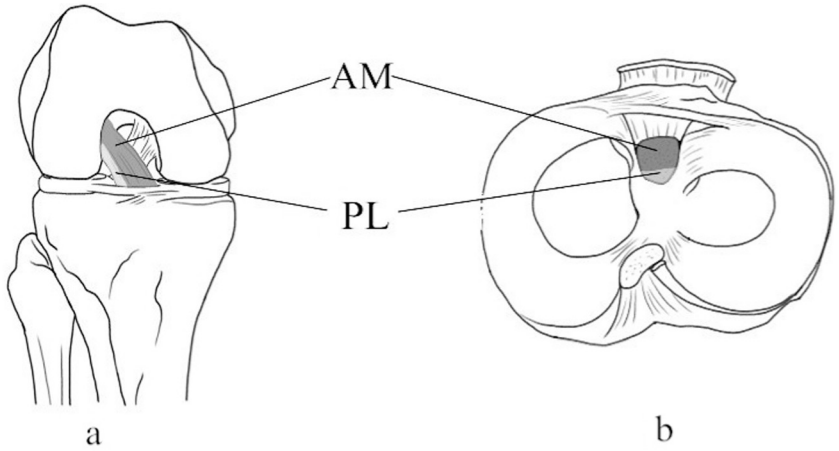

Fig. 1. a. Schematic drawing of the fiber arrangement of the ACL bundles: anteromedial (AM) and posterolateral (PL) bundles.
b. Schematic drawing of the attachment of the ACL bundles.
Left: the flexed right knee joint anterior view. Right: condyles of the right tibial superior view.

The ACL is one of the most frequently injured ligaments of the knee [7,8] with an annual incidence of 8–81 per 100,000 people [9–12]. Partial tears account for 10%–28% [13] of these injuries and most cases result from noncontact pivoting stress during athletic performance when the knee joint is rotated or translated [14]. However, as incidence refers only to cases treated with surgery [15], these statistics may underestimate the actual rate of injury.

When the ACL is injured, reconstruction is often required [9,16]. The goals of anatomical reconstruction of the ACL are to restore its dimensions, collagen orientation, and bundle insertion site [17]. Knowledge of the ACL anatomy, its insertion site and how the injury has altered these is essential to successful treatment. Magnetic resonance imaging (MRI) is the most useful method for obtaining information on the location and extent of an injury associated with bone and soft-tissue structures [18]. However, the utility of conventional orthogonal sagittal MRI is diminished when evaluating partial ACL tears or when the anatomy of the double bundle structure is unknown [1,19]. Exploring an ideal imaging method for ACL evaluation remains a key area of research [1,20–22]. Only a complete description of the presence, insertion location, size, and shape of the two bundles can enable the distinction of the partial tearing and fracture patterns of ACL with MRI and thereby provide anatomical guidance for reconstruction [23]; if the rupture patterns are discerned prior to surgery, the surgical reconstruction of the two bundles can be performed according to their respective conditions [1,24]. It is important for the patient to restore normal knee function and kinematics [16].

Routine MRI examination of the knee consists of spin-echo sequences obtained in sagittal, coronal, and axial planes. However, the oblique course of the ACL renders its visualization via standard orthogonal plane difficult. Many studies have suggested that additional oblique sagittal and coronal MRI views enable better delineation of the course of the ACL rather than the orthogonal views alone [25–27]: Do-Dai [25] reported that the appropriate orientation for oblique imaging was parallel to the outer border of the lateral femoral condyle, Buckwalter [28] found that a 15-degree external rotation of the knee provided the optimal orientation and others [29] reported that the best orientation was a 10- to 20-degree external rotation of the knee. The variance of such recommendations underscores the need for scan-specific for obtaining oblique views of the ACL anatomy via MRI.

Although ACL attachments can be identified via two-dimensional (2D) MRI, slice thickness theoretically limits out-of-plane accuracy and the 2D planes lack information about the spatial relationships of ACL fiber bundles. If the slice thickness in routine MRI sequences is decreased to improve visibility, the consequent low signal-to-noise ratio (SNR) would diminish the image quality. Moreover, multiple planes – or on occasion optimal oblique or double-oblique imaging planes - are required to accommodate for the variability in the positioning of the structures; this results in a lower throughput and longer scanning times [30]. A three-dimensional (3D) isotropic image with multiplanar reformatted images can reduce the total scanning time by removing the need to acquire the same sequence in different planes [31]. 3D fast imaging with steady-state acquisition (3D FIESTA) sequence obtains high signals from tissues with large T2/T1 ratios, such as fluid, blood, and fat [32], and has been used to identify cranial nerves [32,33]. Furthermore, recent advances in MRI technology allow for the acquisition of isotropic voxels, enabling multiplanar reformats of 3D-FIESTA sequences and the reconstruction of images in any plane from the original data [18]. The technique, therefore, enables visualization of the bundles from multiple directions and soft-tissue structures adjacent to bony structures. Despite these advantages, general reconstruction methods have failed to capture the entire, curved length of the ACL. This investigation sought to address this deficiency. We therefore determined the feasibility of the rotating stretched curved planar reconstruction (CPR) of 3D-FIESTA sequence for evaluating the native ACL and its components, AM bundle and PL bundle, in healthy volunteers.

2. Materials and methods

2.1. Patient population

Our sample was comprised of 40 right knees of 40 healthy volunteers (20 males, 20 females, mean age: 23.5 years, age range: 20–29 years) with no history of knee injury or surgery. Physical examinations were performed by a senior orthopaedic surgeon in all cases; the volunteers with positive results on the Lachman or pivot shift tests were excluded from our study. Written informed consent was obtained from each volunteer, and this study was approved by the institutional review board of our hospital (IRB number: QDFY2012007).

2.2. MRI of the ACL

Imaging was performed with a clinical 3.0-T MR scanner (GE Signa HDx, Milwaukee, Wisconsin, USA) equipped with a dedicated knee coil. The protocol consisted of oblique sagittal SE T1WI, coronal FS-PDWI, axial FS-FSE-T2WI, and 3D FIESTA sequences. After obtaining an axial localizer in the supine position, a 2D oblique sagittal SE T1WI MR image was obtained in the plane parallel to the medial border of the lateral femoral condyle (Fig. 2). The sagittal 3D FIESTA of the knee was then obtained. The data consisted of extremely thin slices (slice thickness: 0.6 mm) with no space between consecutive specimens and could

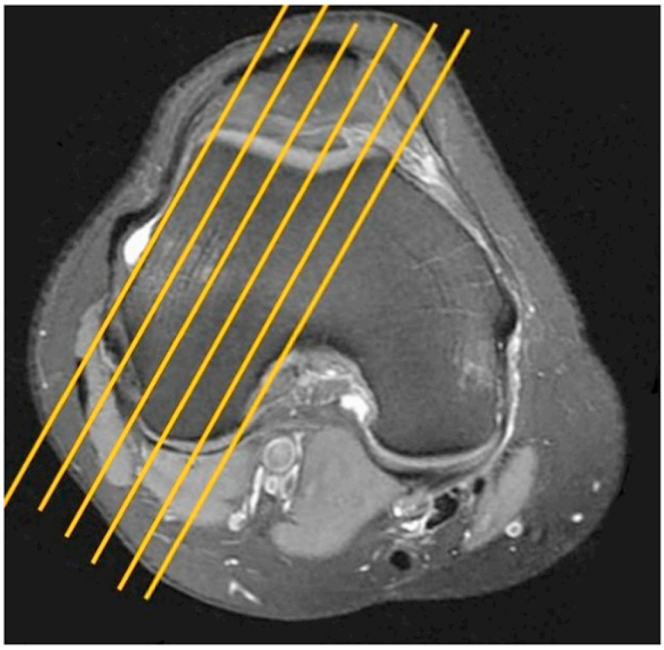

Fig. 2. The axial image scanned by 3 T-MRI using the SE T1WI sequence in 28-year-old man. The oblique sagittal SE T1WI was acquired after an axial scout scan. Slice orientation was placed to parallel to the medial margin of the lateral femoral condyle.

Fig. 3. The sagittal image scanned by 3T-MRI using the curved planar reconstruction(CPR)of 3D-FIESTA in 28-year-old man. The reconstruction line was traced along the course of ACL.

be reconstructed in any plane without degrading the imaging quality. Images of 3D FIESTA were reformatted on a commercially available workstation (Advantage Windows 4.3, GE Healthcare). Rotating stretched CPR were generated. For CPR imaging, we drew a line that followed the curvature of the ACL (Fig. 3). The reconstruction of the ACL line was rotated in increments of 30°. It took < 1.5 min for the radiologists who were familiar with the reformation process.

The parameters for imaging were as follows: (1) oblique sagittal SE T1WI: TR, 520 ms; TE, 11 ms; slice thickness, 3 mm; interslice gap, 1 mm; image acquisition time, 1 min 25 s; FOV, 16 × 16 cm; matrix, 320 × 224; NEX, 2. (2) coronal FS-PDWI: TR, 2000 ms; TE, 15 ms; slice thickness, 4 mm; interslice gap, 1 mm; image acquisition time, 2 min 28 s; FOV, 18 × 18 cm; matrix, 320 × 192; NEX, 2; (3) axial FS-FSE-T2WI: TR, 3400 ms; TE, 102 ms; slice thickness, 5 mm; interslice gap, 0.5 mm; image acquisition time, 1 min 56 s; FOV, 15 × 15 cm; matrix, 320 × 224; NEX, 2; (4) 3D FIESTA: TR, 4.4 ms; TE, 1.7 ms; slice thickness, 0.6 mm; image acquisition time, 4 min 53 s; FOV, 16 × 16 cm; matrix, 256 × 256; NEX, 2.

Fig. 4. The protocol used oblique sagittal spin echo (SE) T1WI sequence as indicated. The oblique sag T1 image includes typical regions of interest drawn for this study labeled with numbers. Two anatomic regions selected for this study are identified: (1) normal bone and (2) normal muscle. Image noise is measured in (3) an artifact free background region.

2.3. MRI Evaluation of the ACL

We evaluated three representative ROIs (Fig. 4) for this study for both sequence images: (1) normal muscle, (2) normal bone, and (3) an artifact-free region within the surrounding air. SNRs and contrast to noise ratios (CNRs) were calculated as follows:

$$SNR_{bone} = SI_{bone}/SD_{air} \quad (1)$$

$$SNR_{muscle} = SI_{muscle}/SD_{air} \quad (2)$$

$$CNR = (SI_{bone} - SI_{muscle})/SD_{air} \quad (3)$$

where SI_{bone} = bone signal intensity at respective sequence, SI_{muscle} = muscle signal intensity at respective sequence, and SI_{air} = standard deviation of background signal.

Images from oblique sagittal SE T1WI and 3D FIESTA CPR were independently evaluated by two observers: an orthopedist with 16 years of experience and a musculoskeletal radiologist with 12 years of experience. The observers were asked to evaluate whether they could discern the femoral end, midportion, tibial end, and the AM and PL bundles of the ACL. The imaging findings were divided into two categories: visible and not visible.

2.4. Statistical analysis

All parameters assessed are presented as means ± SD. Absolute and relative differences of SNR and CNR were calculated for comparison of

different sequence techniques under investigation. Data comparison was performed using Students' paired 2-tailed *t*-test and significance was assumed at P levels of < 0.05. To account for multiple comparisons, a Bonferroni correction was applied.

We further compared the sensitivity of both methods for visualizing different parts of the ACL. Statistical analyses were performed with the SPSS 11.5 for Windows software (SPSS Inc., Chicago, Illinois, USA). Kappa statistics were used to explore the agreement between the observations of the two observers. Fisher's least significant difference (LSD)post hoc test was used for determining the visibility of ACL in different MRI sequences.

3. Results

The ACL SNR efficiency of 3D-FIESTA sequences was 25 ± 3, while that of oblique sagittal T1WI was 17 ± 5 ($P < 0.01$). The CNRs between the ACL and synovial fluid with 3D-FIESTA and oblique sagittal T1WI were 68 ± 5 and 5 ± 3 ($P < 0.001$), respectively.

The femoral end and midportion of the ACL could be visualized using 3D FIESTA sequences in all 40 subjects. On the other hand, the femoral end and midportion of the ACL could not be obtained for 30 and 24 subjects, respectively, with the oblique sagittal SE T1WI ($P < 0.001$). While the double bundles of the ACL could not be visualized with the SE T1WI in any of the subjects, these could be visualized with the CPR of 3D FIESTA sequences in 32 subjects ($P < 0.001$). The tibial end of ACL was obtained for all 40 subjects with the 3D FIESTA sequences and oblique sagittal SE T1WI ($P > 0.05$). These results are presented in Table 1.

CPR of 3D-FIESTA MR imaging was rated superior to the oblique sagittal SE T1WI sequence in 60% and 65% of the cases with regard to the tibial attachment and midportion of the ACL, respectively ($P < 0.05$). CPR of 3D-FIESTA MR imaging was rated superior to the oblique sagittal SE T1WI sequence in 80% and 85% of the cases with regard to the femoral attachment and double bundles of the ACL, respectively ($P < 0.05$).

4. Discussion

The most important finding of our study shows that the rotating stretched CPR of 3D FIESTA can display the entire course of ACL, as well as its anatomical relationships to the surrounding structures. In addition, the imaging technology enabled a non-invasive distinction process of the AM and PL bundles and revealed the spatial distribution of the fiber bundle arrangement, suggesting its potential applications to basic research.

After Palmer [34] first described the AM and PL bundles of the ACL, the double-bundle ACL fibers have been reported in several other studies that used 2D MR [19,20,35]. More recent research has built upon such reports by evaluating the ligament using different isotropic imaging sequences, such as 3D WE-DESS [36], 3D-FSE-Cube [15], 3D MEDIC GRE [37], and 3D VISTA [2,27,38]. To the best of our knowledge, the present study was the first to use the stretched CPR of 3D FIESTA to visualize the entire length of the ACL. Similar to the aforementioned 3D sequences, the 3D-FIESTA sequence can provide isotropic images; such data can be reformatted to view the ACL along its course and reconstructed from an arbitrary plane [2]. Furthermore, the images reformatted with isotropic data are superior to and feature a higher inherent spatial resolution than the 2D planes at typically thicker slices in the direct imaging plane [39].

In diagnostic medical imaging, high SNR and CNR can allow for higher conspicuity of even subtle lesions. Routine MR sequences cannot maintain the benefit of the high SNR and CNR when capturing the ACL; to obtain the whole ligament, the required slice thickness would lower the SNR and CNR. The present study demonstrated that the FIESTA sequence demonstrated a highly significant increase in SNR, yielding better results and overall diagnostic impression relative to SE T1WI [40–42].

Nezahat et al. [43] have confirmed that the 3D FIESTA is an ultrafast pulse sequence that produces high-resolution images with outstanding image contrast between the cerebrospinal fluid, vessels, and CNs and high SNR; small structures are thus made conspicuous. The FIESTA is included in the steady-state free precession sequence and produces signal contrast based on the ratio of T2 to T1 [44,45]. This imaging sequence yields high signals from tissues with large T2/T1 ratios, such as blood and fat [32,46]. FIESTA can therefore enable identification of ligaments because of the excellent fluid-ligament contrast and high spatial resolution. These factors may account for the significant results of the study.

In addition, acquisition of an isotropic 3D FIESTA data set and subsequent image reconstruction along different oblique imaging planes provides a more economical alternative to conventional MRI protocols [15] as it is based on the less time-intensive imaging of steady-state free precession [45,47]. Our mean scan time for the FIESTA image was approximately 4 min 53 s, excluding the time for reformation; and the total scan time for oblique sagittal, coronal, and axial ACL views on 2D FSE was almost 6 min. In order to depict the ligament in its entire length, additional sequences in two or three planes may be required [25], thus increasing scanning time. Nevertheless, the total imaging time for the 3D sequence is considerably less than that for the routine 2D MRI protocol for detecting the ACL within the knee joint [31,48]. Besides, the 3D data can be reconstructed into any desired plane by drawing a line in the data set, precluding the need for repeat imaging. This technique would further allow radiologists to depend less on MRI technologists for obtaining a scan in the proper plane and permit them to make post-scan adjustments to obtain the best view. This technique is not difficult for radiologists to operate. Besides, it would not take much time (< 1.5 min) to do this job.

Although the 3D FIESTA features several advantages, the optimal method for depicting the ligament has hitherto been unexplored. We, therefore, applied the technique of the rotating stretched CPR to obtain visualization of the ACL bundles. It has been used to visualize tubular structures such as blood vessels as rotating the longitudinal section around the central-axis provides the possibility of inspecting the entire vessel [49]. The present study presents a rotating stretched CPR from seven different viewing directions. The reconstruction of the ACL line is rotated at increments of 30° along the rotation axis, which was drawn prior to reconstruction according to the curvature of the ACL. The ACL becomes visible at the angles of 0°, 30°, 60°, 90°, 120°, 150°, and 180° (Fig. 5). We can thus obtain various serial curved slices along the course of the ACL, depicting 2D images of the ACL structure at different angles.

The direct detection of any angle permitted by the curved reconstruction technique enables the visualization of adjacent tissue. Thin contiguous slices and multiplanar reformatting applied to MRI improved the visibility of the precise configuration and location of the ACL and its relation to adjacent bone. Moreover, it provides better anatomic evaluation than do orthogonal views because it permits the

Table 1
Success rates of 3D FIESTA and oblique sagittal SE T1WI in visualizing different parts of the ACL.

Location	Group[a]	3D-FIESTA		Oblique sagittal SE T1WI	
		Number	%	Number	%
Femoral end	1	40	100	10	25
	2	0	0	30	75
Midportion	1	40	100	16	40
	2	0	0	24	60
Tibial end	1	40	100	40	100
	2	0	0	0	0
Double bundles	1	32	80	0	0
	2	8	20	40	100

[a] Group 1: visible; Group 2: not visible.

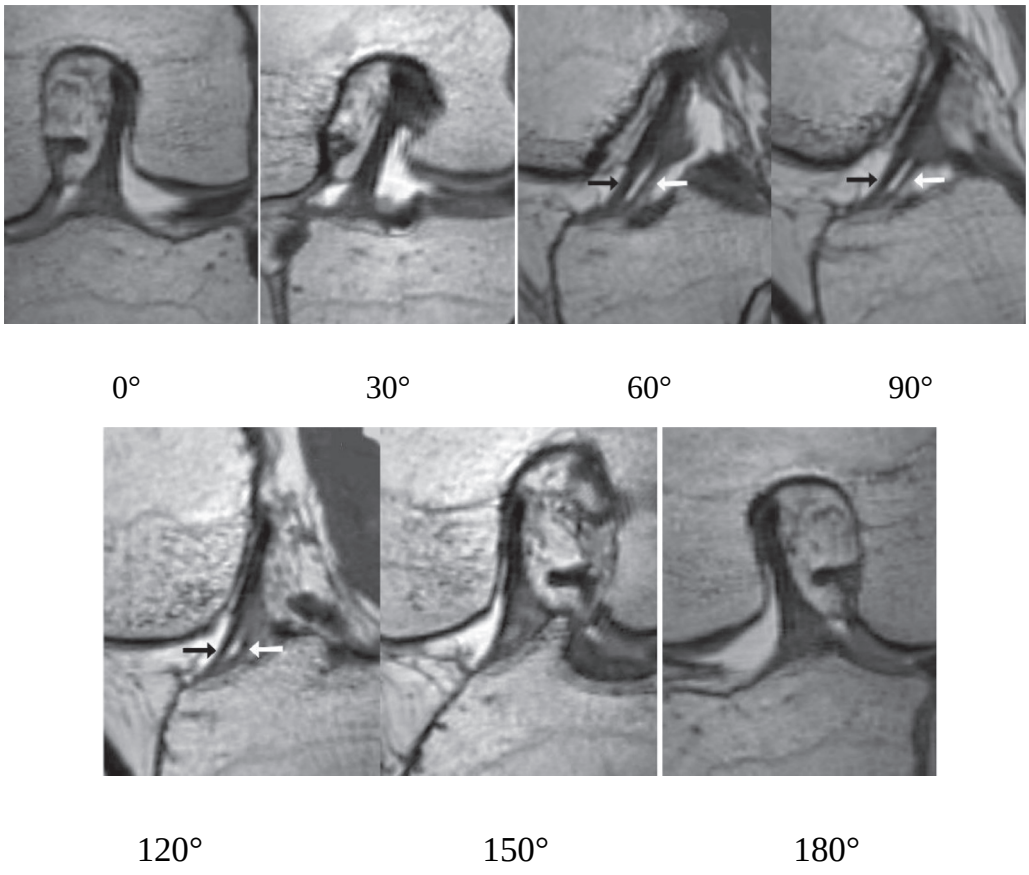

Fig. 5. The CPR of the ACL at the angles of 0°, 30°, 60°, 90°, 120°, 150°, and 180°. Using the Stretched CPR, the reference plane along the course of ACL was formed. By rotating the longitudinal section around the central-axis, the ACL is depicted in its entirety from seven different viewing directions. And it can show the anteromedial (*black arrow*) and the posterolateral (*white arrow*) bundles of the ACL clearly.

evaluation of anatomic details from an arbitrarily chosen orientation. This method allows for the visualization of entire structures with minimal modification of the original data. Moreover, the fiber bundles were most clearly depicted in the rotating stretched CPR of the ACL in the slightly tibial side, from the midpoint between the tibial attachment site and the femur attachment site of the ACL; this was found across all cases. The technique of the rotating stretched CPR with the use of MRI provides a novel way to study the other ligaments.

This study is subject to several limitations. First, only healthy volunteers were included in this study and we cannot determine the efficacy of this technique for displaying an injured ligament. Therefore, the suitability of 3D FIESTA images for the evaluation of pathology, postoperative repair, graft, and ACL reconstruction should be explored in future studies. Another limitation of the present study is the absence of a fat-suppression method. This feature would improve the identification of abnormalities of ligaments. Finally, we could not blind the evaluators to the imaging technique because the 3D images had less sharp margins than the 2D images. This awareness of the image category could have influenced the results.

5. Conclusion

The rotating stretched CPR of 3D-FIESTA sequences is significantly better than conventional 2D-MRI in evaluating the native ACL and its components, AM and PL bundles, in healthy volunteers.

Appendix A. Supplementary data

Supplementary data to this article can be found online at https://doi.org/10.1016/j.mri.2018.09.013.

References

[1] Steckel H, et al. 2D and 3D 3-tesla magnetic resonance imaging of the double bundle structure in anterior cruciate ligament anatomy. Knee Surg Sports Traumatol Arthrosc 2006;14(11):1151–8.
[2] Park HJ, et al. Three-dimensional isotropic T2-weighted fast spin-echo (VISTA) knee MRI at 3.0 T in the evaluation of the anterior cruciate ligament injury with additional views: comparison with two-dimensional fast spin-echo T2-weighted sequences. Acta Radiol 2016;57(11):1372–9.
[3] Petersen W, Zantop T. Anatomy of the anterior cruciate ligament with regard to its two bundles. Clin Orthop Relat Res 2007;454:35–47.
[4] Zantop T, et al. Tunnel positioning of anteromedial and posterolateral bundles in anatomic anterior cruciate ligament reconstruction: anatomic and radiographic findings. Am J Sports Med 2008;36(1):65–72.
[5] Zelle BA, et al. Double-bundle reconstruction of the anterior cruciate ligament: anatomic and biomechanical rationale. J Am Acad Orthop Surg 2007;15(2):87–96.
[6] Pedoia V, et al. Three-dimensional MRI-based statistical shape model and application to a cohort of knees with acute ACL injury. Osteoarthr Cartil 2015;23(10):1695–703.
[7] Lee S, et al. Anterior cruciate ligament reconstruction with use of autologous quadriceps tendon graft. J Bone Joint Surg Am 2007;89(Suppl. 3):116–26.
[8] Hui C, et al. A validation study of a novel 3-dimensional MRI modeling technique to identify the anatomic insertions of the anterior cruciate ligament. Orthop J Sports Med 2016;4(12):232596711667379.
[9] Gianotti SM, et al. Incidence of anterior cruciate ligament injury and other knee ligament injuries: a national population-based study. J Sci Med Sport 2010;12(6):622–7.
[10] Ducouret E, et al. Tunnel positioning assessment after anterior cruciate ligament reconstruction at 12 months: comparison between 3D CT and 3D MRI. A pilot study. Orthop Traumatol Surg Res 2017;103(6):937–42.
[11] Kothari A, et al. Evaluating rotational kinematics of the knee in ACL reconstructed patients using 3.0Tesla magnetic resonance imaging. Knee 2012;19(5):648–51.
[12] Clayton RAE, Court-Brown CM. The epidemiology of musculoskeletal tendinous and ligamentous injuries. Injury 2008;39(12):1338–44.
[13] Tjoumakaris FP, Donegan DJ, Sekiya JK. Partial tears of the anterior cruciate ligament: diagnosis and treatment. Am J Orthop 2011;40(2):92–7.
[14] Breitenseher MJ, Mayerhoefer ME. Oblique MR imaging of the anterior cruciate ligament based on three-dimensional orientation. J Magn Reson Imaging 2007;26(3):794–8.
[15] Lefevre N, et al. Partial tears of the anterior cruciate ligament: diagnostic performance of isotropic three-dimensional fast spin echo (3D-FSE-Cube) MRI. Eur J Orthop Surg Traumatol 2014;24(1):85–91.

[16] Tashiro Y, et al. Anterior cruciate ligament tibial insertion site is elliptical or triangular shaped in healthy young adults: high-resolution 3-T MRI analysis. Knee Surg Sports Traumatol Arthrosc 2017;26(2):485–90.
[17] Fu FH, et al. Anatomic anterior cruciate ligament reconstruction: a changing paradigm. Knee Surg Sports Traumatol Arthrosc 2015;23(3):640–8.
[18] Pass B, et al. Can a single isotropic 3D fast spin echo sequence replace three-plane standard proton density fat-saturated knee MRI at 1.5 T? Br J Radiol 2015;88(1052):20150189.
[19] Duc SR, et al. Magnetic resonance imaging of anterior cruciate ligament tears: evaluation of standard orthogonal and tailored paracoronal images. Acta Radiol 2005;46(7):729–33.
[20] Barberie J, et al. Oblique sagittal view of the anterior cruciate ligament: comparison of coronal vs. axial planes as localizing sequences. J Magn Reson Imaging 2001;14(3):203.
[21] Hong SH, et al. Grading of anterior cruciate ligament injury. Diagnostic efficacy of oblique coronal magnetic resonance imaging of the knee. J Comput Assist Tomogr 2003;27(5):814–9.
[22] Katahira K, et al. MR imaging of the anterior cruciate ligament: value of thin slice direct oblique coronal technique. Radiat Med 2001;19(1):1–7.
[23] Rahmer J, Bornert P, Dries SP. Assessment of anterior cruciate ligament reconstruction using 3D ultrashort echo-time MR imaging. J Magn Reson Imaging 2009;29(2):443–8.
[24] Carpenter RD, Majumdar S, Ma CB. Magnetic resonance imaging of 3-dimensional in vivo tibiofemoral kinematics in anterior cruciate ligament-reconstructed knees. Art Ther 2009;25(7):760–6.
[25] Do-Dai DD, Stracener JC, Youngberg RA. Oblique sagittal MRI of anterior cruciate ligament. J Comput Assist Tomogr 1994;18(1):160–2.
[26] Kwon JW, et al. Which oblique plane is more helpful in diagnosing an anterior cruciate ligament tear? Clin Radiol 2009;64(3):291–7.
[27] Woo Yi J, et al. Usefulness of the oblique view of three-dimensional isotropic T2-weighted fast spin-echo (VISTA) in the evaluation of anterior cruciate ligament reconstruction. Clin Imaging 2016;40(4):610–6.
[28] Buckwalter KA, Pennes DR. Anterior cruciate ligament: oblique sagittal MR imaging. Radiology 1990;175(1):276–7.
[29] Engeler C, Miller S, Ochsner EG. Oblique sagittal MR imaging of the anterior cruciate ligament. Radiology 1991;178(3):890–1.
[30] Yoon YC, et al. Diagnostic efficacy in knee MRI comparing conventional technique and multiplanar reconstruction with one-millimeter FSE PDW images. Acta Radiol 2007;48(8):869–74.
[31] Kijowski R, et al. Knee joint: comprehensive assessment with 3D isotropic resolution fast spin-Echo MR imaging-diagnostic performance compared with that of conventional MR imaging at 3.0 T. Radiology 2009;252(2):486–95.
[32] Schmitz B, Hagen T, Reith W. Three-dimensional true FISP for high-resolution imaging of the whole brain. Eur Radiol 2003;13(7):1577–82.
[33] Mikami T, et al. Cranial nerve assessment in posterior fossa tumors with fast imaging employing steady-state acquisition (FIESTA). Neurosurg Rev 2005;28(4):261–6.
[34] Palmer I. On the injuries to the ligaments of the knee joint: a clinical study. 1938. Clin Orthop Relat Res 2007;454:17–22. [discussion 14].
[35] Cohen SB, et al. MRI measurement of the 2 bundles of the normal anterior cruciate ligament. Orthopedics 2009;32(9).
[36] Rajeswaran G, Lee JC, Healy JC. MRI of the popliteofibular ligament: isotropic 3D WE-DESS versus coronal oblique fat-suppressed T2W MRI. Skelet Radiol 2007;36(12):1141–6.
[37] Swami VG, et al. Reliability of 3D localisation of ACL attachments on MRI: comparison using multi-planar 2D versus high-resolution 3D base sequences. Knee Surg Sports Traumatol Arthrosc 2014;23(4):1206–14.
[38] Lee JE, et al. Evaluation of selective bundle injury to the anterior cruciate ligament: T2-weighted fast spin-Echo 3-T MRI with reformatted 3D oblique isotropic (VISTA) versus 2D technique. AJR Am J Roentgenol 2017;209(5):W308–16.
[39] Otsubo H, et al. MRI depiction and 3D visualization of three anterior cruciate ligament bundles. Clin Anat 2017;30(2):276–83.
[40] Wintersperger BJ, et al. Brain tumor enhancement in MR imaging at 3 tesla: comparison of SNR and CNR gain using TSE and GRE techniques. Investig Radiol 2007;42(8):558.
[41] Stinson EG, et al. Dixon-type and subtraction-type contrast-enhanced magnetic resonance angiography: a theoretical and experimental comparison of SNR and CNR. Magn Reson Med 2015;74(1):81–92.
[42] Steckner MC, Liu B, Ying L. A new single acquisition, two-image difference method for determining MR image SNR. Med Phys 2009;36(2):662–71.
[43] Erdogan N, et al. MRI assessment of internal acoustic canal variations using 3D-FIESTA sequences. Eur Arch Otorhinolaryngol 2012;270(2):469–75.
[44] Amano Y, et al. Magnetic resonance portography using contrast-enhanced fat-saturated three-dimensional steady-state free precession imaging. J Magn Reson Imaging 2004;19(2):238–44.
[45] Nitz W. Fast and ultrafast non-echo-planar MR imaging techniques. Eur Radiol 2002;12(12):2866.
[46] Zhou Q, et al. Preoperative demonstration of neurovascular relationship in trigeminal neuralgia by using 3D FIESTA sequence. Magn Reson Imaging 2012;30(5):666–71.
[47] Kornaat PR, et al. MR imaging of articular cartilage at 1.5 T and 3.0 T: comparison of SPGR and SSFP sequences 1 2. Osteoarthr Cartil 2005;13(4):338–44.
[48] Stevens KJ, et al. Ankle: isotropic MR imaging with 3D-FSE-cube-initial experience in healthy volunteers. Radiology 2008;249(3):1026–33.
[49] Kanitsar A, et al. CPR: curved planar reformation. Visualization, 2002. 2002.